© 2016. Published by The Company of Biologists Ltd | Journal of Cell Science (2016) 129, 3562-3573 doi:10.1242/jcs.190017

RESEARCH ARTICLE

TRIM17 contributes to autophagy of midbodies while actively sparing other targets from degradation

Michael A. Mandell[1,*], Ashish Jain[2,3,4], Suresh Kumar[1], Moriah J. Castleman[1], Tahira Anwar[5], Eeva-Liisa Eskelinen[5], Terje Johansen[3], Rytis Prekeris[6] and Vojo Deretic[1,*]

ABSTRACT

TRIM proteins contribute to selective autophagy, a process whereby cells target specific cargo for autophagic degradation. In a previously reported screen, TRIM17 acted as a prominent inhibitor of bulk autophagy, unlike the majority of TRIMs, which had positive roles. Nevertheless, TRIM17 showed biochemical hallmarks of autophagy-inducing TRIMs. To explain this paradox, here, we investigated how TRIM17 inhibits selective autophagic degradation of a subset of targets while promoting degradation of others. We traced the inhibitory function of TRIM17 to its actions on the anti-autophagy protein Mcl-1, which associates with and inactivates Beclin 1. TRIM17 expression stabilized Mcl-1–Beclin-1 complexes. Despite its ability to inhibit certain types of selective autophagy, TRIM17 promoted the removal of midbodies, remnants of the cell division machinery that are known autophagy targets. The selective loss of anti-autophagy Mcl-1 from TRIM17–Beclin-1 complexes at midbodies correlated with the ability of TRIM17 to promote midbody removal. This study further expands the roles of TRIMs in regulating selective autophagy by showing that a single TRIM can, depending upon a target, either positively or negatively regulate autophagy.

KEY WORDS: HIV, Mcl-1, Midbody, Selective autophagy, Tripartite-motif

INTRODUCTION

Autophagy is mechanism of cellular waste elimination involving the delivery of cytoplasmic targets, including protein aggregates, damaged organelles and pathogens, to the lysosome for degradation (Khaminets et al., 2015; Lazarou et al., 2015; Gomes and Dikic, 2014; Pampliega et al., 2013). In the most-studied form of autophagy, macroautophagy, the cytoplasmic cargo is sequestered within a double-membrane delimited organelle termed an autophagosome, which then fuses with lysosomes, resulting in the degradation of its luminal contents (Mizushima et al., 2011). As autophagy plays numerous key homeostatic functions in the cell, its misregulation can be detrimental to cellular health, and both insufficient and excessive autophagy have been shown to contribute to various pathological states (Fulda and Kogel, 2015; Mizushima and Komatsu, 2011).

Because of the cellular need to optimize autophagic activity, the autophagy pathway is subject to extensive regulation (Popelka and Klionsky, 2015). Signals regulating autophagy initiation, the stage at which the initial membrane rearrangements take place that lead to autophagosome formation, converge on the human VPS34 (also known as PIK3C3) complex (Mizushima et al., 2011). This complex generates phosphatidylinositol 3-phosphate (PI3P) on membranes at sites of autophagosome biogenesis (Kihara et al., 2001), leading to the recruitment of other components of the autophagy machinery (Obara et al., 2008; Dooley et al., 2014). The key regulatory component of the complex in mammalian cells is Beclin 1 (Liang et al., 1999). Under autophagy 'on' conditions, Beclin 1 is ubiquitylated on K63 (Shi and Kehrl, 2010) and/or phosphorylated by the Ser/Thr kinases including MK2 and MK3 (also known as MAPKAPK2 and MAPKAPK3) (Wei et al., 2015), AMPK (Kim et al., 2013) and ULK1 (Russell et al., 2013), the latter of which is itself subject to positive or negative regulation by upstream kinases such as AMPK or the mTOR complex (Kim et al., 2011; Egan et al., 2011). In many cases, protein platforms facilitate the interaction between Beclin 1 and its regulatory partners, as exemplified by the exocyst, which brings ULK1 and Beclin 1 together during starvation-induced bulk autophagy (Bodemann et al., 2011). Under autophagy 'off' conditions, Beclin 1 is held in an inactive state through interactions with inhibitory binding partners such as TAB2 (Criollo et al., 2011; Takaesu et al., 2012) or certain members of the Bcl-2 family of proteins including Bcl-2 (Pattingre et al., 2005) and Mcl-1 (Tai et al., 2013; Germain et al., 2011; Erlich et al., 2007). In addition to having roles in autophagy initiation, Beclin 1 also contributes to the maturation of autophagosomes into autolysosomes. This process is also regulated at several levels, with at least some of the regulation again centered on Beclin 1, as the interactions of Beclin 1 with UVRAG or Rubicon respectively promote or inhibit maturation (Matsunaga et al., 2009; Zhong et al., 2009). Autophagy is also regulated at a transcriptional level by TFEB and other MiT or TEF transcription factors, coordinating autophagy-inducing stimuli with the expression of genes involved in autophagy or lysosome biogenesis (Settembre et al., 2011), whereas the transcription factor ZKSCAN3 inhibits their expression (Chauhan et al., 2013).

Another approach to autophagy regulation is at the level of substrate specificity, whereby only selected targets are degraded. As the result of intensive study, we are now beginning to understand how the autophagic apparatus recognizes specific targets (Randow and Youle, 2014). A general feature of this process is the presence of receptors such as p62 (also known as sequestosome 1, SQSTM1) that bridge the substrate to mammalian Atg8 homologs (mAtg8s),

[1]Department of Molecular Genetics and Microbiology, University of New Mexico Health Sciences Center, 915 Camino de Salud, Albuquerque, NE NM 87131 USA. [2]Molecular Cancer Research Group, Institute of Medical Biology, University of Tromsø – The Arctic University of Norway, Tromsø 9037, Norway. [3]Department of Molecular Cell Biology, Institute for Cancer Research, Oslo University Hospital, Montebello, Oslo N-0379, Norway. [4]Center for Cancer Biomedicine, Faculty of Medicine, University of Oslow, Montebello, Oslo N-0379, Norway. [5]Department of Biosciences, University of Helsinki, Helsinki 00014, Finland. [6]Department of Cell and Developmental Biology, University of Colorado School of Medicine, 12801 East 17th Avenue, Aurora, CO 80045, USA.

*Author for correspondence (mmandell@salud.unm.edu; vderetic@salud.unm.edu)

M.A.M., 0000-0002-5773-2806

Received 31 March 2016; Accepted 13 August 2016

Journal of Cell Science (2016) 129, 3562-3573 doi:10.1242/jcs.190017

such as LC3B (also known as MAP1LC3B), associated with the autophagosomal membrane (Birgisdottir et al., 2013; Rogov et al., 2014). Although our understanding of the players involved in selective autophagy is growing, we know less about how the process of selective autophagy is linked with autophagy regulation and how some targets of selective autophagy are degraded while other potential selective autophagy targets are spared.

Recent studies have implicated the TRIM family of proteins (Reymond et al., 2001) as both autophagy receptors that directly bind to their substrates (Kimura et al., 2015; Mandell et al., 2014; Niida et al., 2010) and as autophagy regulators (Kimura et al., 2015; Mandell et al., 2014; Barde et al., 2013; Yang et al., 2013), thus potentially being positioned to couple target specificity with autophagy induction or inhibition (Kimura et al., 2016). Several TRIMs such as TRIM5α, TRIM6, TRIM20, TRIM21 and others have been demonstrated to promote autophagy by assembling the key autophagy regulators ULK1 and Beclin 1 in their activated states (Kimura et al., 2015; Mandell et al., 2014). In contrast to these autophagy-promoting TRIMs, TRIM17 (also known as Terf; testis ring finger) is notable because its knockdown dramatically increases the number of autophagosomes in cells, suggesting that TRIM17 can inhibit autophagy (Mandell et al., 2014). However, initial investigations into the mode of action of TRIM17 unexpectedly have indicated that it retains many characteristics of pro-autophagy TRIMs including mAtg8 binding and organization of ULK1–Beclin-1 complexes (Mandell et al., 2014). Here, we show that the apparent dichotomy in TRIM17 autophagic actions result from it having dual roles. TRIM17 protects a variety of selective autophagy targets from degradation while also contributing to the elimination of midbodies, known selective autophagy substrates consisting of the tightly packaged remnants of the cell division machinery.

RESULTS

TRIM17 inhibits degradation of selective autophagy targets

We first tested how TRIM17 knockdown using multiple small interfering RNAs (siRNAs) affected the abundance of p62 by performing high-content imaging (Fig. 1A–C). We found that TRIM17 siRNAs reduced the amount of total p62 (Fig. 1B) in HeLa cells. Cells subjected to TRIM17 siRNAs also had fewer p62 puncta (Fig. 1C), structures associated with polyubiquitylated protein aggregates destined for autophagic degradation (Pankiv et al., 2007). We also assessed the abundance of p62 and of the autophagy-associated lipidated form of LC3B (known as LC3-II) by immunoblotting (Fig. 1D). We again observed that the abundance of p62 was reduced in TRIM17 knockdown cells (Fig. 1E). Treatment of these cells with an inhibitor of autophagosome maturation (bafilomycin A1) rescued the protein levels of p62, indicating that TRIM17 expression reduces the autophagic degradation of p62. TRIM17 knockdown did not significantly affect the abundance of LC3-II (Fig. 1F). The effects of TRIM17 knockdown were independent of the stringency of the lysis buffer used (Fig. 1G).

The above results indicate that TRIM17 inhibits the autophagic degradation of p62. Accordingly, TRIM17 expression increased the abundance of p62 structures in cells leading to, at times, a striking aggregation of p62 (Fig. 1H). TRIM17 expression also prevented p62 degradation in cells treated with pp242, a drug that induces autophagy through mTOR inhibition (Fig. 1I). We next tested whether TRIM17 could interfere with autophagic degradation of a range of other reported targets for selective autophagy. Certain proteins associated with primary ciliogenesis, including IFT20 and OFD1, have been reported to undergo degradation by autophagy (Pampliega et al., 2013; Tang et al., 2013). Accordingly, we found that both IFT20 and OFD1 levels in cells were increased following autophagy inhibition with bafilomycin A1 (Fig. 1J). When TRIM17 was expressed in these cells, IFT20 levels were similarly increased and the effects of bafilomycin A1 on IFT20 levels were abrogated, suggesting that TRIM17 prevents the selective autophagic degradation of IFT20. We did not detect effects of TRIM17 expression on OFD1 or on ZWINT, another protein previously reported to interact with TRIM17 (Endo et al., 2012). Additionally, we did not detect an effect of bafilomycin treatment on the protein levels of GFP–TRIM17, indicating that TRIM17 itself is not a target of autophagy (Fig. 1I,J).

As another example of a selective autophagy target, we tested whether TRIM17 could affect the autophagic targeting of TRIM5α, which has recently been reported to be protected from lysosomal degradation by autophagy inhibition (Imam et al., 2016). In agreement with these findings, mCherry–eYFP–TRIM5α showed primarily ‘red’ and not green fluorescence in cells, indicating its presence within acidified compartments (Fig. 2A) (Klionsky et al., 2016). Inhibition of autophagic maturation by bafilomycin increased the signal from the pH-sensitive eYFP. We found that TRIM17 was in protein complexes with TRIM5α in cells and also co-immunoprecipitated TRIM22 (Fig. 2B), in keeping with the previously reported observations that TRIM17 colocalizes with TRIM5α and TRIM22 (Mandell et al., 2014). TRIM17 expression reduced the colocalization between GFP–TRIM5α and LC3B puncta (Fig. 2C), and GFP–TRIM5α and GFP–TRIM22 levels were increased when co-expressed with mCherry–TRIM17 (Fig. 2D,E), indicating that TRIM17 protects certain TRIMs from proteolysis.

In conjunction with the known anti-retroviral activities of TRIM5α (Stremlau et al., 2004; Pertel et al., 2011), we have reported that rhesus TRIM5α (RhTRIM5α) functions as an autophagic receptor promoting degradation of the HIV-1 capsid protein p24 (Mandell et al., 2014). Given that autophagy receptors are typically co-degraded with their cargo (Johansen and Lamark, 2011), we reasoned that TRIM17-mediated protection of TRIM5α might also protect p24 from autophagic degradation. Whereas expression of GFP–RhTRIM5α in HEK293T cells reduced the abundance of cellular p24 at 3 hours following infection with VSV-G pseudotyped HIV-1 relative to cells expressing GFP alone (Fig. 2F), co-expression of mCherry–TRIM17 prevented both degradation of GFP–RhTRIM5α (as described above) and that of HIV-1 p24 to levels exceeding those in cells expressing GFP alone. Thus, TRIM17 expression blocked the RhTRIM5α- and autophagy-dependent degradation of capsid protein. The observation that TRIM17 increased levels of p24 above what was seen in control cells (Fig. 2D, compare left and right lanes) suggests that additional human proteins might act as receptors promoting autophagic degradation of the HIV-1 capsid, although less efficiently than RhTRIM5α. Collectively, these data show that TRIM17 is a broad, albeit not universal, inhibitor of selective autophagy.

TRIM17 assembles Mcl-1–Beclin-1 complexes

We next sought to determine how TRIM17 interferes with autophagy, and considered several possibilities. TRIM17 puncta colocalized with the lysosomal marker LAMP2 (Fig. 3A). Under autophagy ‘off’ conditions, TFEB localizes to lysosomes (Settembre et al., 2012). Thus, we considered the possibility that TRIM17 might suppress TFEB nuclear translocation to inhibit autophagy. TRIM17 knockdown did not alter the nuclear translocation of TFEB under basal or induced autophagy conditions (Fig. 3B).

Journal of Cell Science (2016) 129, 3562-3573 doi:10.1242/jcs.190017

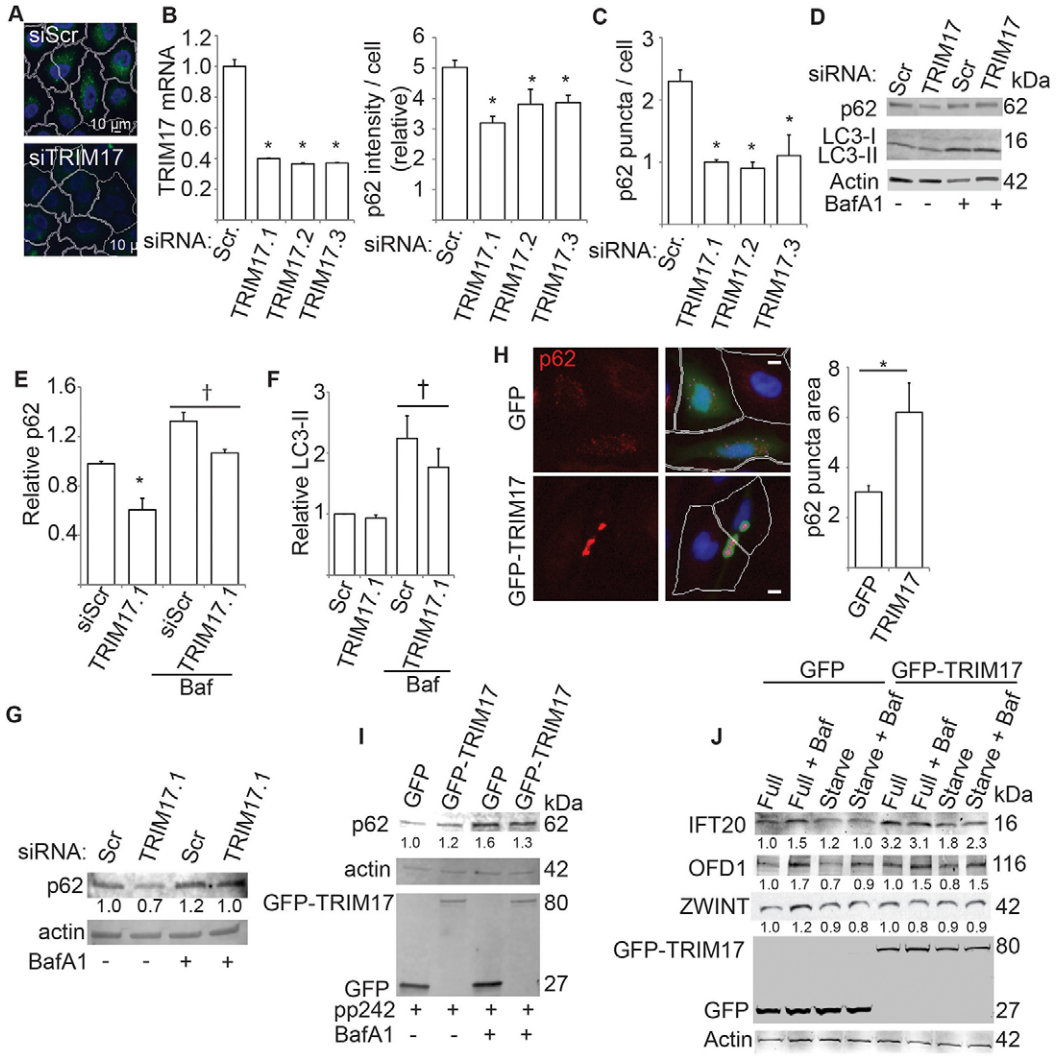

Fig. 1. TRIM17 expression reduces selective autophagy. (A) Representative epifluorescent microscopy image from high-content imaging analysis of p62 (green) in HeLa cells subjected to TRIM17 siRNA (siTRIM17) or scramble control siRNA (siScr). White lines indicate automatically determined cell boundaries. (B) Left, knockdown efficiency of TRIM17 assessed by qPCR following transfection with different siRNA oligonucleotides. Right, the average intensity of anti-p62 signal per cell as determined by high-content imaging following control or TRIM17 knockdowns in HeLa cells. Data are means±s.e.m., *n*=3 experiments. **P*<0.05 (ANOVA with Bonferroni *post hoc* test). (C) Quantification of the average number of p62 puncta per cell as determined by high-content imaging following control or TRIM17 knockdowns in HeLa cells. Data are means±s.e.m., *n*=3 experiments. **P*<0.05 (ANOVA). (D–F) Effect of TRIM17 knockdown on the levels of LC3-II and p62. (D) Immunoblot analysis of the abundance of the indicated proteins following TRIM17 or control knockdown and culture in the presence or absence of bafilomycin A1 (BafA1) in full medium conditions. Quantification of relative p62 (E) or LC3-II abundance (F) as determined by densitometry. Data are means± s.e.m., *n*=3 experiments. **P*<0.05; †*P*>0.05 (ANOVA). (G) Cells were treated as in D prior to lysis under more stringent conditions (RIPA buffer). (H) High-content imaging analysis of the effects of GFP–TRIM17 expression on the abundance of p62-positive structures. Cells were automatically identified based on nuclear staining, and then cells showing above-background levels of GFP or GFP–TRIM17 fluorescence were analyzed for the total area of p62 structures (red) per cell. White lines, cell boundaries. Purple structures in the right image indicate p62-positive structures identified by automated image analysis. Data are means±s.e.m., *n*=3 experiments. **P*<0.05 (*t*-test). Scale bars: 10 µm. (I) Immunoblot analysis of the effect of TRIM17 expression on the abundance of p62 in cells treated with the autophagy inducer pp242 in the presence or absence of bafilomycin A1. Values underneath the p62 row indicate the relative abundance as determined by densitometry. (J) Effects of TRIM17 expression protects on IFT20, OFD1 and ZWINT protein levels. Lysates from HEK293T cells were transfected with GFP or GFP–TRIM17 and subjected to the indicated treatments (Full, full medium; Starve, starvation medium; Baf, BafA1 treatment) for 2 h were probed for the indicated proteins by immunoblotting. Numbers underneath the rows indicate the relative abundance as determined by densitometry.

Because TRIM5α and TRIM20 have been reported to preferentially associate with the key autophagy regulator ULK1 in its active phosphorylated form (phosphorylated on Ser317) (Kimura et al., 2015; Mandell et al., 2014), we next tested whether TRIM17 preferentially bound to active or inactive (phosphorylated on Ser757) phospho-ULK1. In these experiments, we also included TRIM22, which we previously identified as a positive regulator of autophagy (Mandell et al., 2014). Given the inhibitory effects of TRIM17 on autophagy noted here, we were surprised to see that it preferentially bound to active phospho-ULK1 (Fig. 3C) similar to autophagy-promoting TRIMs. Thus, our experiments with TFEB nuclear translocation or phospho-ULK1 do not help explain the inhibitory effects of TRIM17 on autophagy.

BH3-domain proteins such as Bcl-2 can act to inhibit autophagy, so we considered a model in which TRIM17 might inhibit autophagy through actions on these proteins. TRIM17 has been reported to interact with the Bcl-2 family protein Mcl-1 (Magiera et al., 2013), a protein with known anti-autophagy functions that are

Journal of Cell Science (2016) 129, 3562-3573 doi:10.1242/jcs.190017

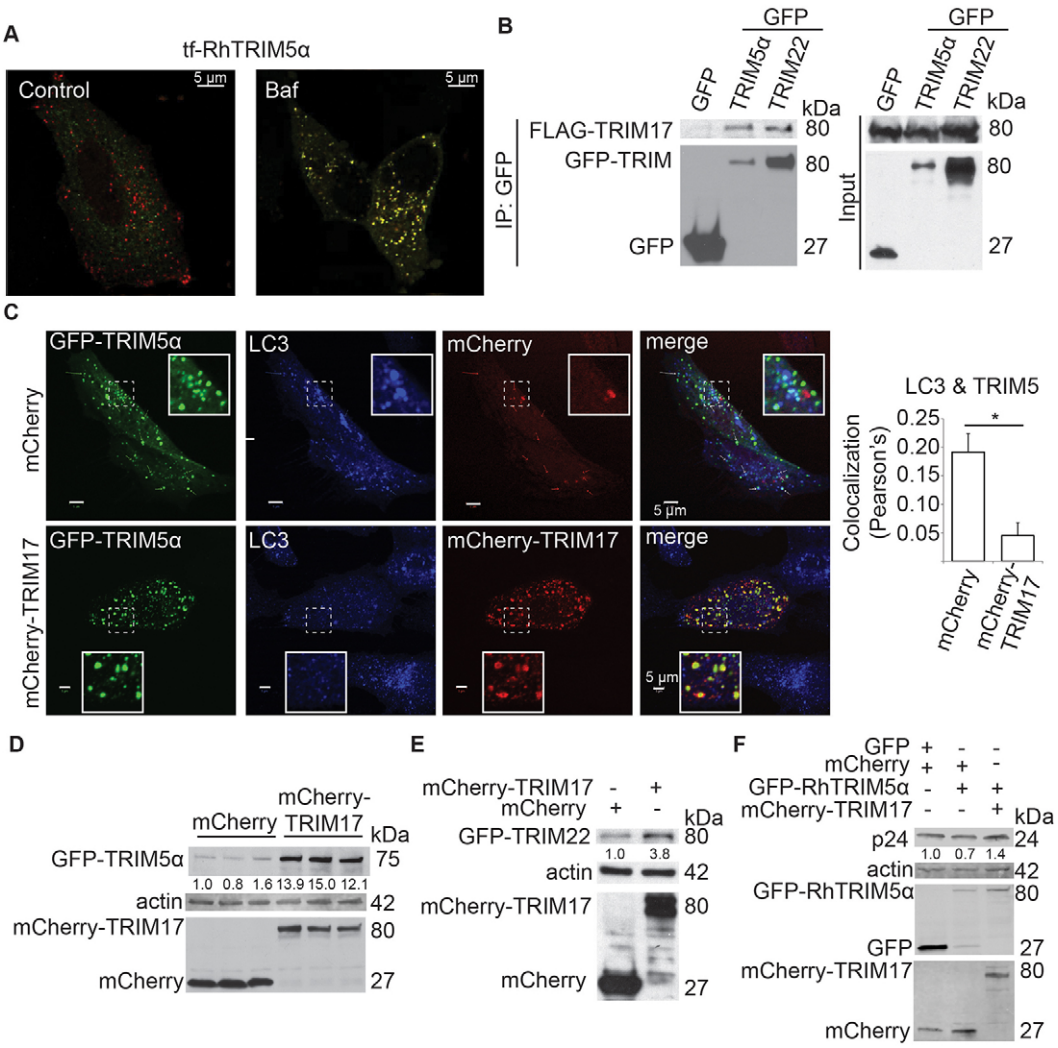

Fig. 2. TRIM17 inhibits autophagic degradation of TRIM5α and HIV-1 capsids. (A) TRIM5α is subject to lysosomal degradation. Tandem-fluorescence mCherry–eYFP-tagged TRIM5α (tfRhTRIM5α; rhesus) yields primarily red fluorescence when expressed in HeLa cells. Bafilomycin A1 (Baf) restores YFP fluorescence by inhibiting autolysosomal acidification. (B) Co-immunoprecipitation (IP) analysis of interactions between TRIM17 and other TRIMs from lysates of transfected HEK293T cells. (C) Confocal microscopic analysis of colocalization between GFP–TRIM5α and endogenous LC3B in HeLa cells transfected with mCherry–TRIM17 or mCherry alone. Insets show enlargements of the indicated area. Right, the Pearson's correlation coefficient (colocalization) was determined from confocal micrographs using image analysis software. Data are means±s.e.m., n=3 experiments. *P<0.05 (t-test). (D,E) Effect of TRIM17 expression on protein levels of GFP-tagged RhTRIM5α (D) or TRIM22 (human; E). Numbers underneath the rows indicate the relative abundance of GFP–TRIM as determined by densitometry. (F) Effect of TRIM17 expression on RhTRIM5α-dependent HIV-1 capsid protein (p24) degradation. HEK293T cells were transfected as indicated and infected with VSV-G pseudotyped HIV-1 for 3 h under conditions of amino acid starvation (EBSS) prior to sample lysis. Numbers underneath the p24 row indicate the relative abundance of p24 as determined by densitometry.

similar to those of Bcl-2 (Pattingre et al., 2005; Wei et al., 2008; Chang et al., 2010). Mcl-1 is proposed to block autophagy through binding to the BH3 domain of Beclin 1 in an inhibitory manner (Erlich et al., 2007), but additional mechanisms have also been reported (Lindqvist et al., 2014). We thus tested whether TRIM17 could recruit Mcl-1 into Beclin 1 complexes. In agreement with our previous results showing that TRIM17 interacts with Beclin 1, we found that the two proteins colocalized to various puncta within cells (Fig. 3D). In contrast, tagged TRIM17 and Mcl-1 did not show any spatial association in colocalization studies (Fig. 3E), with Mcl-1 showing a predominantly diffuse pattern in contrast to the pattern of small puncta and large structures shown by TRIM17. However, when TRIM17, Mcl-1, and Beclin 1 were all co-expressed in cells, Mcl-1 was recruited into TRIM17–Beclin-1 puncta (Fig. 3F), suggesting that Beclin 1 might contribute to the formation of TRIM17–Mcl-1 complexes, a model that we tested by co-immunoprecipitation (Fig. 4A,B). Although we could detect Mcl-1–TRIM17 protein complexes in cells, the addition of exogenous Beclin 1 expression increased the abundance of these complexes. Similarly, TRIM17 expression increased the interaction between Mcl-1 and Beclin 1 (Fig. 4C,D). Taken together, these data show that TRIM17 serves as an assembly platform for Beclin 1 with its negative regulator Mcl-1.

We next tested whether Mcl-1 was important for TRIM17-dependent p62 accumulation. As expected, cells transfected with control siRNA and expressing GFP–TRIM17 had more p62-positive structures relative to cells expressing GFP alone (Fig. 4E). When Mcl-1 expression was knocked down by siRNA, GFP–TRIM17 was attenuated in its ability to increase the abundance of these p62 structures. These data indicate that the TRIM17-interacting partner Mcl-1 contributes to the anti-autophagy activities of TRIM17.

Journal of Cell Science (2016) 129, 3562-3573 doi:10.1242/jcs.190017

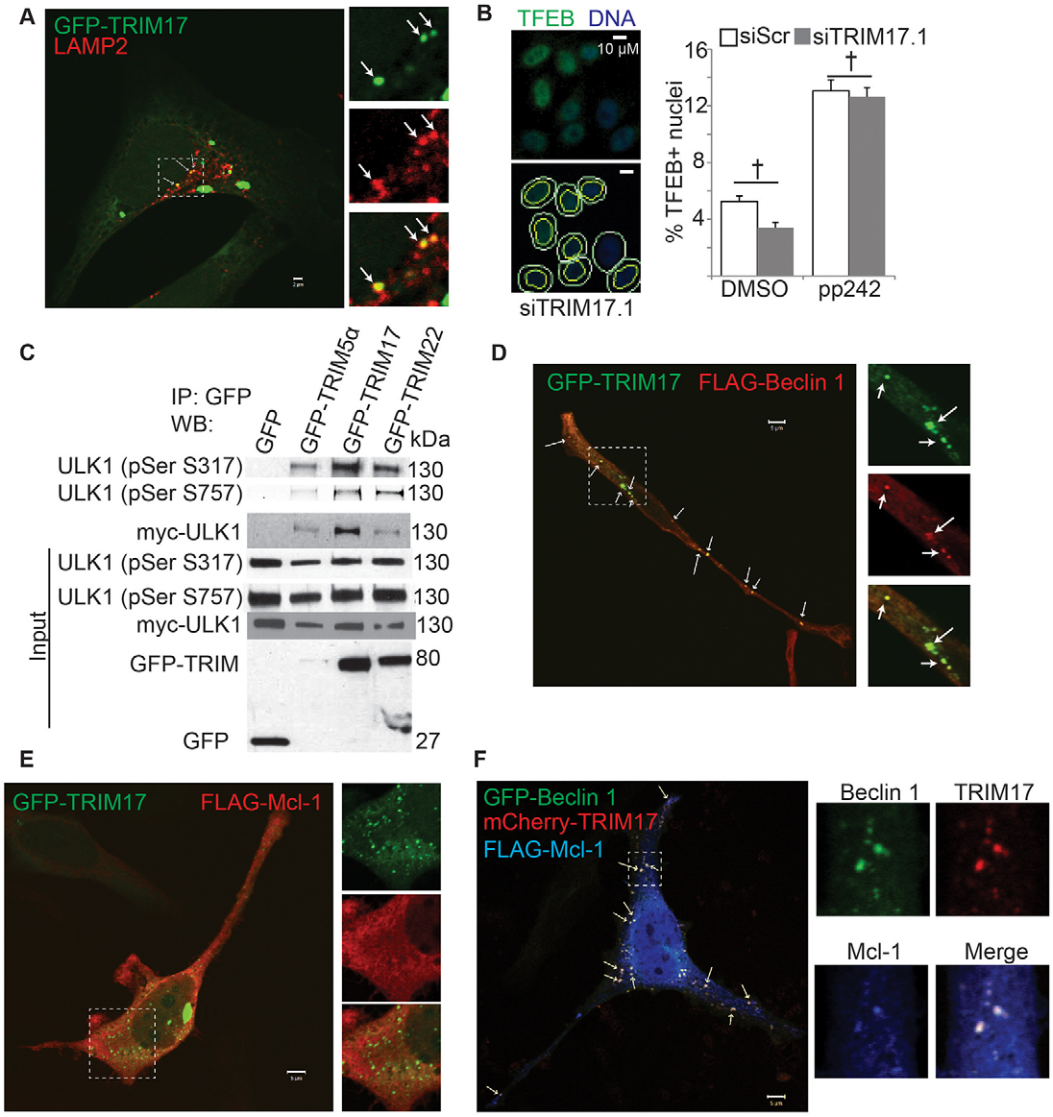

Fig. 3. TRIM17 and Beclin 1 colocalize with the anti-autophagy factor Mcl-1. (A) Confocal microscopic analysis of the GFP–TRIM17 and LAMP2 localization in HeLa cells. Arrows indicate colocalizing puncta. (B) High-content imaging analysis of TFEB nuclear translocation. Left, representative image of HeLa cells subjected to TRIM17 knockdown (siTRIM17.1), treated with pp242, and stained to detect TFEB and DNA. The bottom image shows the cell boundary (whites line) and TFEB-positive nuclei (yellow line). Right, the percent of nuclei showing TFEB-positivity under the indicated conditions. siScr, scrambled siRNA. Data are means±s.e.m., n=3 experiments. $^{\dagger}P$>0.05 (ANOVA). (C) Co-immunoprecipitation (IP) analysis of interactions between TRIMs and active (pSer317) versus inactive (pSer757) phospho-ULK1 from the lysates of transfected HEK293T cells as assessed by western blotting (WB). (D) Confocal microscopic analysis of the GFP–TRIM17 and FLAG–Beclin-1 localization in HeLa cells. Arrows indicate colocalizing puncta. (E) Confocal microscopic analysis of the GFP–TRIM17 and FLAG–Mcl-1 localization in HeLa cells. (F) Confocal microscopic analysis of the mCherry–TRIM17, Beclin-1–GFP and FLAG–Mcl-1 localization in transfected HeLa cells. Arrows indicate colocalizing puncta. Enlargements of the indicated area in A, D E and F are shown on the right of the main images.

TRIM17 promotes midbody removal by autophagy

Despite negatively regulating the degradation of several autophagy targets, in some respects TRIM17 has features suggestive of a positive-acting role in autophagy. These include (1) direct binding to a subset of mAtg8s and p62 (Mandell et al., 2014), and (2) the ability to assemble ULK1 and Beclin 1 into a complex (Mandell et al., 2014), with the ULK1 interacting with TRIM17 being preferentially in its active phospho-form (Fig. 3C). We found that a subset of TRIM17 structures colocalize with punctate substrates positive for p62 (Fig. 5A) and ubiquitin (Fig. 5B). These structures, which are removed from cells by autophagy (Pankiv et al., 2007), have an aggregate-like appearance in electron microscopy studies (Bjorkoy et al., 2005). Accordingly, ultrastructural analysis of TRIM17-demarcated cytoplasmic regions with correlative light electron microscopy showed that TRIM17 localized to such aggregates (Fig. 5C). Finally, a subset of TRIM17 structures colocalized with the autophagosome marker LC3B (Fig. 6A), suggesting further that TRIM17 might also positively affect autophagy under some circumstances, possibly in a substrate-dependent manner.

In a search for such putative targets, we considered the midbody ring. Midbodies are dense protein structures containing the remnants of the cell division machinery. They are formed at the site of abscission and are inherited by one of the two daughter cells. Previous studies (Isakson et al., 2013; Kuo et al., 2011; Pohl and Jentsch, 2009) have shown that midbodies colocalize with LC3B, with the autophagy receptors p62 and NBR1, and with the autophagy adaptor ALFY (also known as WDFY3). Knockdown

Journal of Cell Science (2016) 129, 3562-3573 doi:10.1242/jcs.190017

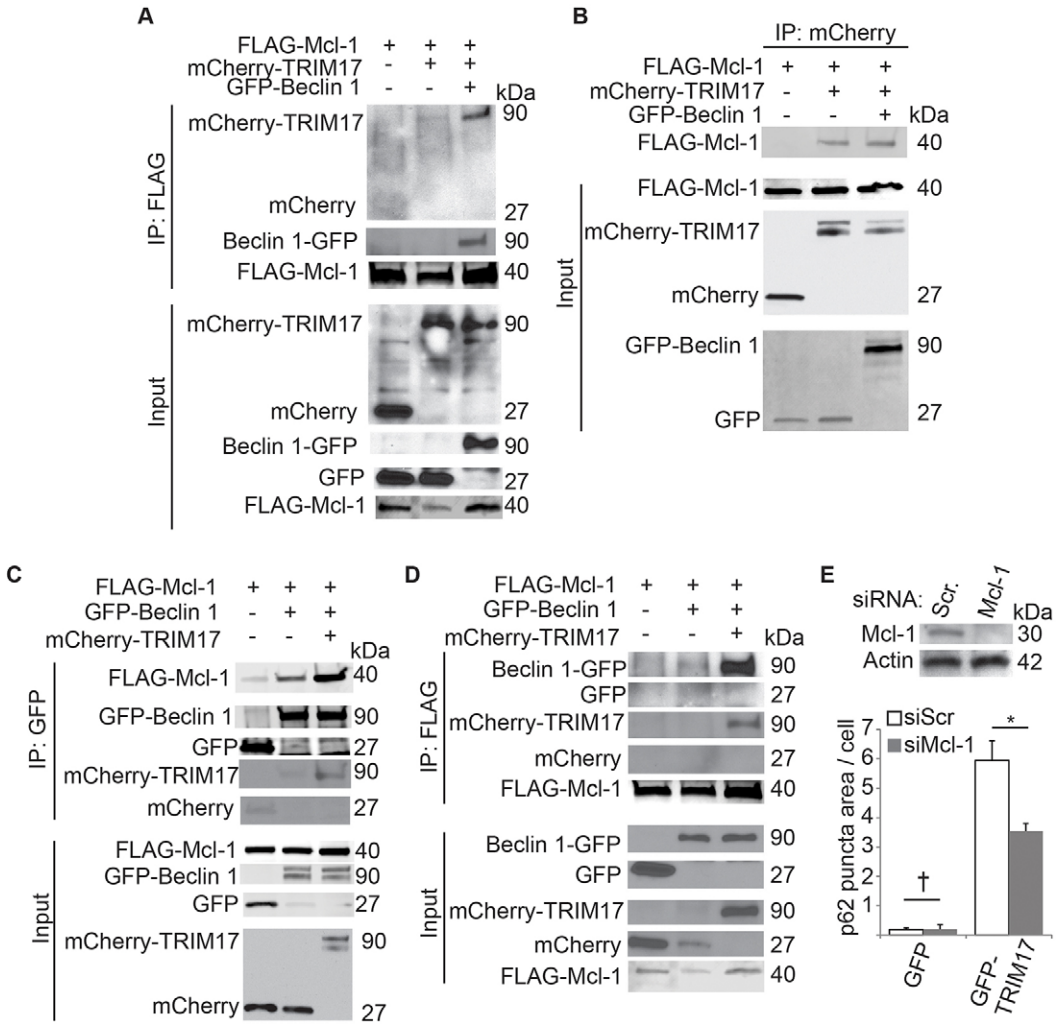

Fig. 4. TRIM17 stabilizes interactions between autophagy factor Beclin 1 and anti-autophagy Mcl-1. (A,B) Co-immunoprecipitation (IP) analysis of the effect of Beclin 1 expression on the abundance of Mcl-1 in TRIM17 protein complexes from lysates of transfected HEK293T cells using anti-FLAG (for Mcl-1; A) or anti-GFP (for Beclin 1; B) antibodies for immunoprecipitation. (C,D) Co-immunoprecipitation analysis of the effect of TRIM17 expression on the abundance of Mcl-1 in Beclin 1 protein complexes from lysates of transfected HEK293T cells using anti-GFP (for Beclin 1; C) or anti-FLAG (for Mcl-1; D) antibodies for immunoprecipitation. (E) Effect of Mcl-1 knockdown on the abundance of p62 puncta in cells expressing GFP alone or GFP–TRIM17. Top, knockdown efficiency of Mcl-1 in HeLa cells. Bottom, HeLa cells were subjected to control (siScr) or Mcl-1 siRNA (siMcl-1) and subsequently transfected with GFP alone or GFP–TRIM17. Fixed samples were stained with anti-p62 prior to automated imaging and analysis. Only cells showing GFP-positivity were analyzed. Data are means±s.e.m., n=5 experiments. *P<0.05; †P>0.05 (ANOVA).

of these proteins or the autophagy factors Beclin 1 or ATG7 led to an accumulation of midbodies, demonstrating that their removal is autophagy dependent. Similar to the above autophagy factors, TRIM17 colocalized with or formed rings around midbodies (recognized here with an antibody against MKLP1, a protein highly concentrated in midbodies; Fig. 6B). We next used high-content imaging to determine what effect TRIM17 knockdown had on the abundance of midbodies (Fig. 6C–F). We found that cells subjected to TRIM17 knockdown contained more midbodies regardless of the TRIM17 siRNA used (Fig. 6D) and that the average size of the midbodies in these cells was larger (Fig. 6E), both indicative of less midbody degradation in the absence of TRIM17. Repeating these experiments in cells stably expressing GFP-tagged MKLP1 yielded similar results (Fig. 6F).

The number of midbodies per cell is dependent in part on the duration of the cell cycle (Pohl and Jentsch, 2009), as midbodies are only generated at the end of cytokinesis. We therefore tested whether the observed effects of TRIM17 knockdown on midbody numbers could be an indirect result of increased midbody production resulting from TRIM17 accelerating the cell cycle. By assessing the DNA content of TRIM17 knockdown cells, we found that a higher percentage of TRIM17 knockdown cells were in S and/or G2 phase than cells transfected with control siRNA (Fig. 6G). Thus, TRIM17 promotes cell division, and its knockdown would be expected to decrease, not increase, the number of midbodies per cell, ruling out the indirect explanation. We also tested to see whether TRIM17 knockdown altered the formation of midbodies at the abscission site, but did not see any effect (Fig. 6H). Taken together, these results show that TRIM17 contributes to the autophagy-dependent removal of midbodies.

TRIM17 and Beclin 1 localize to midbodies, but Mcl-1 is excluded

Given the inhibitory effect of TRIM17 on the degradation of other autophagy targets, we wondered how TRIM17 could promote the autophagic degradation of midbodies. As was the case with

Journal of Cell Science (2016) 129, 3562-3573 doi:10.1242/jcs.190017

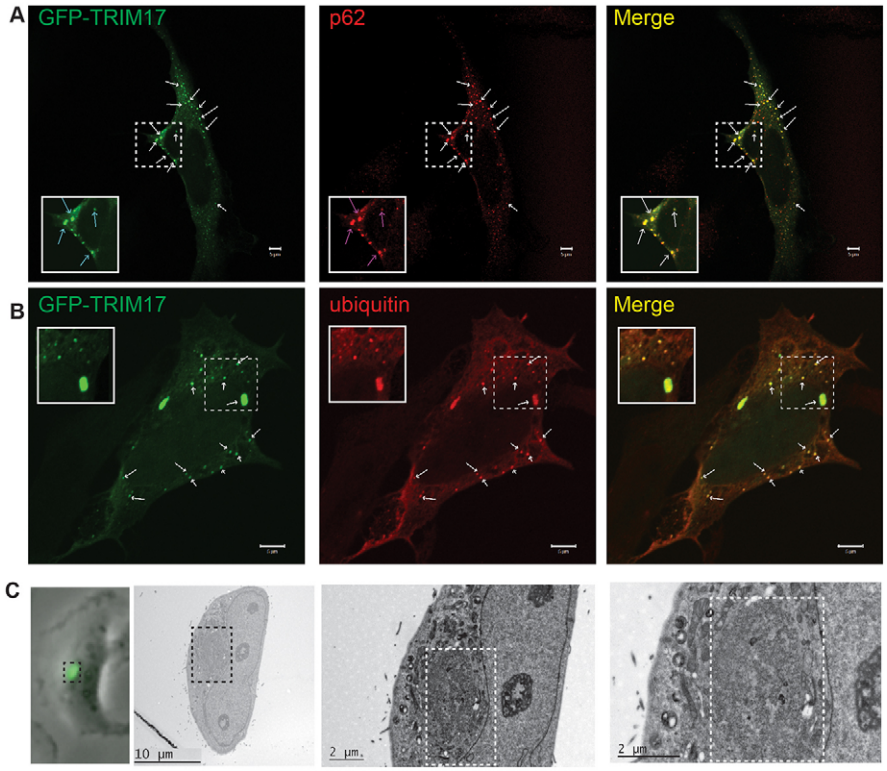

Fig. 5. TRIM17 colocalizes with autophagic substrates. (A) Confocal microscopic analysis of the localization of GFP–TRIM17 and endogenous p62 in HeLa cells. Arrows indicate colocalizing puncta. (B) Confocal microscopic analysis of the localization of GFP–TRIM17 and endogenous ubiquitin in HeLa cells. Arrows indicate colocalizing puncta. Insets show enlargements of the indicated area. (C) Correlative-light electron microscopic analysis of GFP–TRIM17-expressing HeLa cells. The boxed area indicates the location of TRIM17 fluorescence.

TRIM17, we found that Beclin 1 also colocalizes with a population of midbodies (Fig. 7A), and that mCherry–TRIM17, Beclin-1–GFP and the midbody marker MKLP1 all colocalized (Fig. 7B). In contrast, we were unable to find instances of FLAG-tagged Mcl-1 colocalizing with MKLP1 (Fig. 7C). Because our previous results indicated that the localization pattern of Mcl-1 is altered when co-expressed with both TRIM17 and Beclin 1, we also tested whether FLAG-tagged Mcl-1 colocalized with MKLP1 in cells simultaneously expressing GFP-tagged Beclin 1 and TRIM17 by performing confocal microscopy (Fig. 7D,E). As expected, in these cells, Mcl-1 had a punctate localization pattern, with Mcl-1 puncta showing robust colocalization with the GFP signal. However, although we readily found instances of GFP-positive midbodies, these were Mcl-1 negative. Furthermore, we were unable to find any Mcl-1 positive midbodies by confocal microscopy. To quantify these relationships, we used high-content imaging to determine the fraction of midbodies positive for GFP signal (TRIM17 and/or Beclin 1) and Mcl-1 (Fig. 7F). We found that a substantially higher percentage of midbodies were associated with TRIM17 and/or Beclin 1 than with Mcl-1. These data suggest a model in which the presence or absence of Mcl-1 determines whether TRIM17 complexes inhibit or promote selective autophagy.

Finally, we considered whether the autophagic removal of midbodies might involve other TRIMs or if this function is specific to TRIM17. To address this, we performed an siRNA screen in which we knocked down a set of 35 TRIMs in HeLa cells and then quantified the number of midbodies per cell by high-content imaging (Fig. 8A,B). As expected, knockdown of autophagy factors LC3B or Beclin 1 increased the number of midbodies per cell. In contrast, and opposite to the effects of TRIM17 knockdown, a high percentage of the TRIM knockdown cells had a reduced the number of midbodies. Three TRIMs stood out at the other end of the spectrum (TRIM21, TRIM47 and TRIM76, the latter is also known as CMYA5) by increasing the number of midbodies per cell by more than three standard deviations above what was seen in cells subjected to non-targeting siRNA. These data suggest that other TRIMs, in addition to TRIM17, contribute to midbody abundance, possibly through effects on the cell cycle as initially considered for TRIM17 above (e.g. the majority of TRIMs tested), whereas the autophagic removal of midbody remnants from cells following cytokinesis might be the function of TRIM17 and possibly of TRIM21, TRIM47 and TRIM76.

DISCUSSION

The purpose of our study was to determine the role of TRIM17 in autophagy, prompted by the previously reported features of TRIM17 (Mandell et al., 2014) that are indicative of both autophagy-promoting and autophagy-inhibiting activities. The principal findings reported here are that TRIM17 inhibits autophagic degradation of diverse known targets, but that at the same time it focuses autophagy on at least one substrate, midbodies. Its autophagy-inhibitory activities involve Mcl-1, which TRIM17 assembles into complexes with the key autophagy regulator Beclin 1. When TRIM17 carries out pro-autophagy activities it is freed from Mcl-1, thus disinhibiting autophagy at defined places.

Midbodies are organelles consisting of the multiple proteins involved in the final steps of cytokinesis, which form at the abscission site and are inherited by one of the two daughter cells. These structures might not be inert, but instead appear to contribute to cellular signaling and affect differentiation, with cells containing elevated numbers of midbodies having more stem cell characteristics (Dionne et al., 2015). Previous studies have shown that autophagy contributes to midbody removal (Isakson et al., 2013; Kuo et al., 2011; Pohl and Jentsch, 2009), collectively indicating that midbodies colocalize with markers of the autolysosomal system (e.g. LC3 proteins) and that knockdowns of autophagy factors (ATG7 or Beclin 1) or receptors (p62, NBR1 and

Journal of Cell Science (2016) 129, 3562-3573 doi:10.1242/jcs.190017

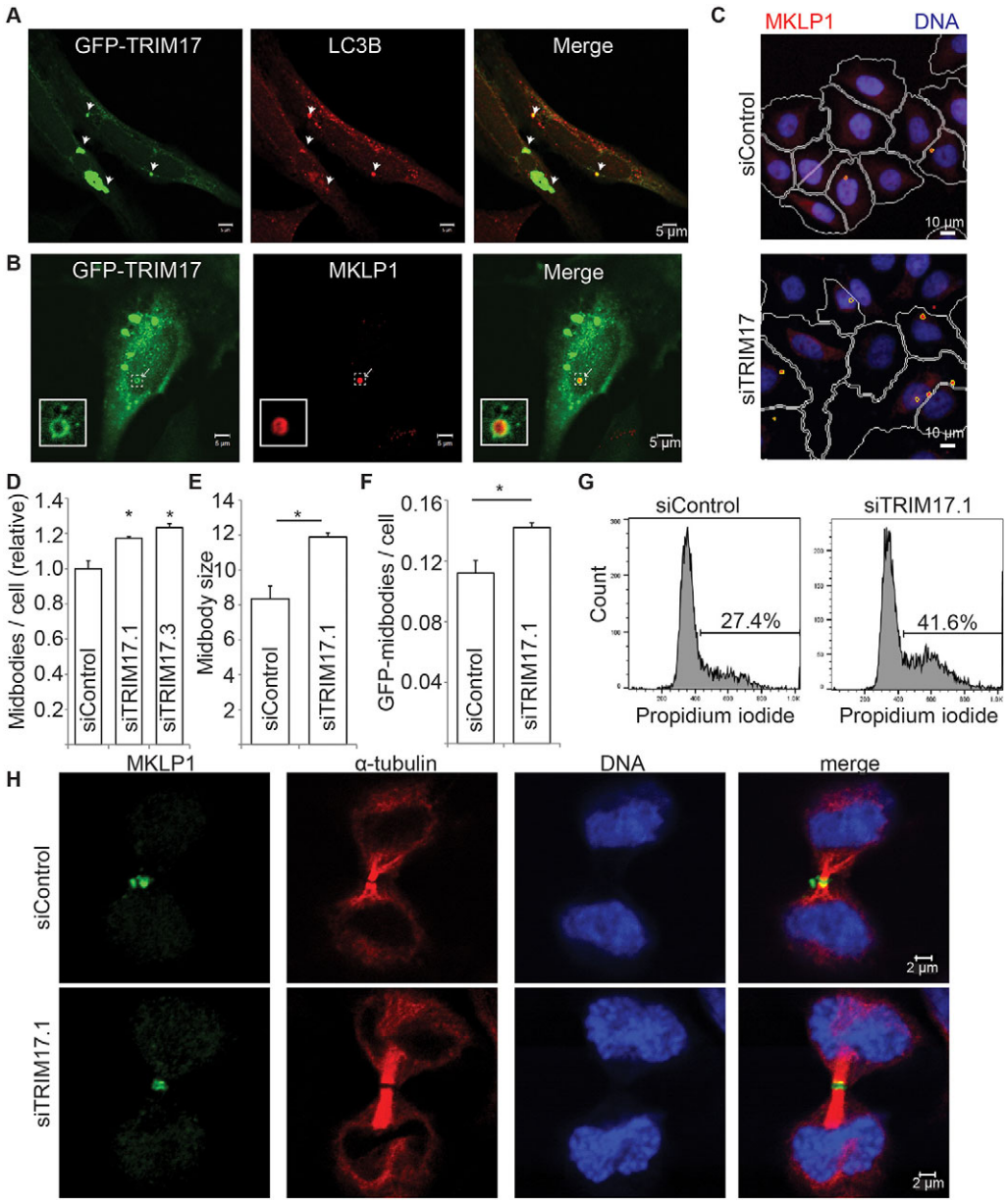

Fig. 6. TRIM17 contributes to midbody degradation through autophagy. (A) Confocal microscopic analysis of GFP–TRIM17 and LC3B localization in HeLa cells. Arrowheads indicate colocalizing puncta. (B) Colocalization analysis of GFP–TRIM17 and the midbody marker MKLP1 in HeLa cells. Insets show enlargements of the indicated area. (C,D) High-content microscopic analysis of the effects of TRIM17 knockdown on midbody abundance. Midbodies were detected in HeLa cells subjected to control (siControl) or TRIM17 knockdown with two separate siRNAs (siTRIM17) and stained with anti-MKLP1 and automatically imaged and analyzed. Top, control siRNA. Bottom, TRIM17 siRNA. Images display machine-determined positions of cell boundaries (white lines) and midbodies (yellow mask). The average number of midbodies per cell was then automatically determined (D). (E) The average size of midbodies was determined in HeLa cells subjected to control or TRIM17 knockdown. (F) HeLa cells stably expressing GFP–MKLP1 were subjected to TRIM17 or control knockdown, and the number of GFP-labeled midbodies per cell was determined by high-content imaging. (G) DNA content of HeLa cells subjected to TRIM17 or control siRNA as determined by propidium iodide staining and flow cytometry. Values shown in G represent the percentage of cells in G2 or S phase. Data, means±s.e.m., $n \geq 3$ experiments. *$P<0.05$ (*t*-test). (H) Localization of midbodies in dividing cells following control or TRIM17 knockdown. HeLa cells were transfected with the indicated siRNA 72 h prior to fixation and labeled for immunofluorescence with the indicated antibodies. Cells undergoing division were identified on the basis of their nuclear morphology and the presence of a tubulin demarcated bridge that links the two daughter cells.

ALFY) can cause midbody accumulation. TRIM17 has the potential to link these separate autophagy-related systems together along with the autophagy-activating kinase ULK1 in its active form, consistent with the concept of 'precision autophagy' proposed for other TRIMs (Kimura et al., 2016). In addition to TRIM17, we identified three other TRIMs (TRIM21, TRIM47 and TRIM76) that also contribute to the autophagic removal of midbodies. TRIM21 (Niida et al., 2010; Kimura et al., 2015) and TRIM76 (Mandell et al., 2014) have been previously linked to autophagy, but little is known about the physiological roles of TRIM47. Nevertheless, these observations indicate a strong association between TRIMs and the control of midbody abundance.

To date, the study of selective autophagy has focused primarily on how presumptive targets of autophagy are identified by receptors that guide the autophagic apparatus to explain how the cell 'decides' what to degrade (Stolz et al., 2014; Rogov et al.,

Journal of Cell Science (2016) 129, 3562-3573 doi:10.1242/jcs.190017

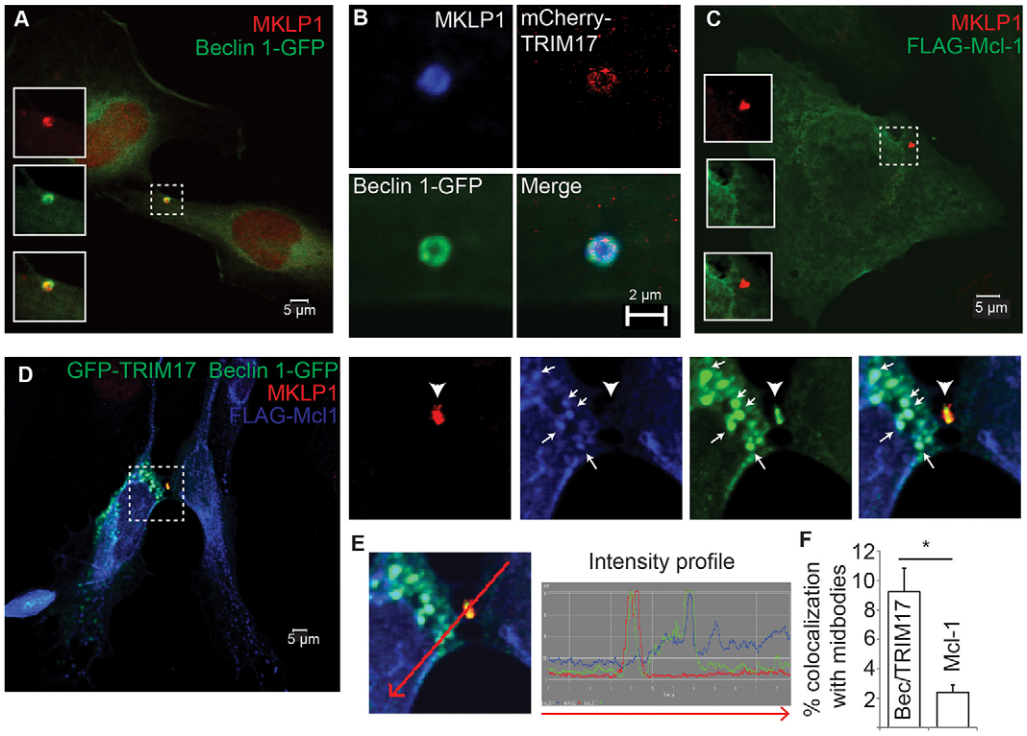

Fig. 7. Mcl-1 is excluded from midbody-localized TRIM17 complexes, and other TRIMs contribute to midbody removal. (A) Confocal microscopic image showing localization of Beclin-1–GFP to midbodies demarcated by anti-MKLP1 staining in HeLa cells. (B) Zoomed-in confocal image of a midbody showing Beclin-1–GFP and mCherry–TRIM17 positivity. (C) Confocal images of a HeLa cell expressing FLAG-tagged Mcl-1 and stained with anti-MKLP1. (D) Confocal microscopic colocalization analysis of Mcl-1 with midbodies in cells expressing GFP–TRIM17 and Beclin-1–GFP. Arrowhead, localization of midbody. Arrows, puncta showing colocalization between GFP signal and FLAG-Mcl-1. Insets in A and C, and right panels of D show enlargements of the indicated area. (E) Fluorescence intensity profile of midbody shown in D. (F) High content microscopic analysis of cells as in D showing the percentage area of midbodies colocalizing with GFP signal (Beclin 1 and/or TRIM17) or Mcl-1 signal. Data are means±s.e.m., n=5 experiments. *P<0.05 (t-test).

2014). Our study suggests that another facet of selective autophagy involves the cell selecting not to degrade certain potential targets. We found that the inhibitory activities of TRIM17 extended to blocking precision autophagy mediated by other TRIMs, as exemplified by its ability to prevent TRIM5α-dependent degradation of HIV-1 capsids. In addition to the interactions between TRIM17 and several TRIMs (TRIM5α and TRIM22) shown here, TRIM17 has also been reported to interact with TRIM44 (Urano et al., 2009). TRIM17 binding to other TRIM family members could similarly interfere with their pro-autophagy functions, thus protecting their cognate substrates from degradation and extending the substrate-protective repertoire of

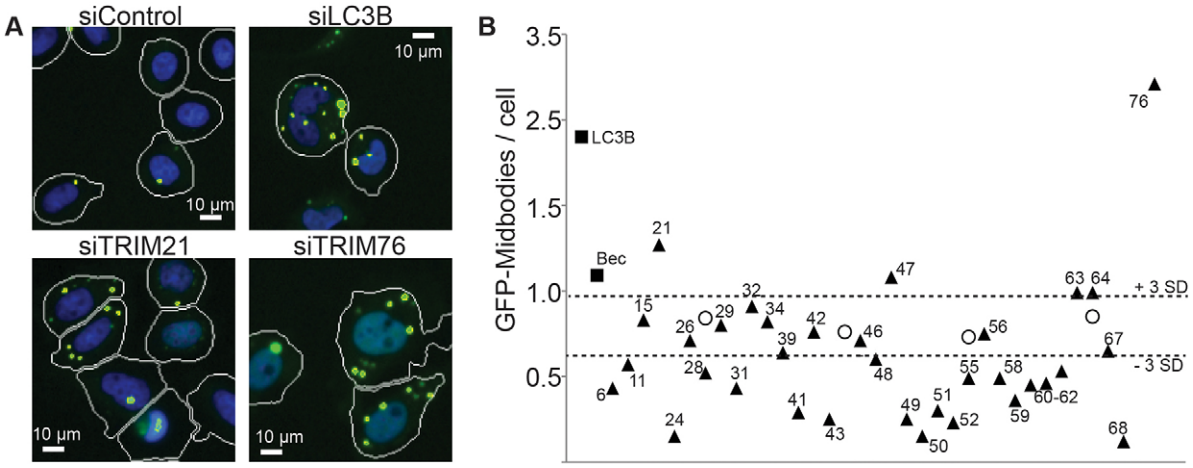

Fig. 8. An siRNA screen reveals that additional TRIMs contribute to midbody degradation. (A,B) siRNA screen for TRIMs affecting midbody abundance. HeLa cells stably expressing GFP–MKLP1 were subjected to the indicated knockdowns (siControl, control siRNA; siLC3B, LC3B siRNA; siTRIM21, TRIM21 siRNA; siTRIM76, TRIM76 siRNA) and the number of midbodies per cell was determined by high-content imaging at 72 h after transfection. Images in A display machine-determined positions of cell boundaries (white lines) and midbodies (yellow mask). Numbers in plot in B (black triangles) are TRIM gene numbers. Black squares, LC3B or Beclin 1 (Bec). Open circles, cells subjected to control siRNA. Dashed lines, three standard deviations (s.d.) above or below mean of controls. One of two experiments is shown.

Journal of Cell Science

TRIM17. TRIM17 might not be the only TRIM that can focus selective autophagy. We identified TRIM76 as contributing to midbody removal. Like TRIM17, TRIM76 was also previously identified as a negative regulator of autophagy (Mandell et al., 2014). Furthermore, TRIM28 (also known as KAP1) has been shown to promote autophagy in two studies (Barde et al., 2013; Yang et al., 2013), yet it is also reported to act in an inhibitory manner (Pineda et al., 2015). In the case of TRIM28, its autophagy-modulating functions appear tied to its E3 ubiquitin ligase activity – a feature shared with most TRIMs. The role of the enzymatic activity of TRIM17, and how it contributes to autophagy control vis-à-vis proteasomal actions, would be of interest to future studies. Given their dual actions in autophagy regulation, TRIM17, TRIM28, TRIM76 and potentially other TRIMs could confer upon the cell an ability to discriminate between autophagic substrates in a 'this-but-not-that' manner, allowing for another layer of specificity in cytoplasmic quality and content control by autophagy.

TRIM17 impacts upon cellular functions in additional ways. First, we observed that TRIM17 regulates cell division, possibly through its interactions with ZWINT (Endo et al., 2012). ZWINT is a component of the kinetochore that is also reported to interact with Beclin 1, although this has not been linked to autophagy (Fremont et al., 2013). Second, we found that the inhibitory actions of TRIM17 on autophagy led to p62 accumulation, and p62 has been shown to affect numerous signaling pathways (Katsuragi et al., 2015). A very recent report shows that these signaling events can be affected by the actions of a TRIM upon p62: TRIM21-dependent ubiquitylation of p62 interferes with the ability of p62 to aggregate and sequester Keap1, a negative regulator of cellular responses to oxidative stress (Pan et al., 2016). TRIM17 expression increases the abundance of p62 aggregates, and so would be expected to have an opposing effect to that of TRIM21.

In conclusion, our study demonstrates a new mechanism whereby a TRIM regulates selective autophagy by promoting the autophagic targeting of some substrates while blocking the targeting of others. These dual and opposing activities of TRIM17, and potentially other TRIMs like TRIM76, might endow cells with enhanced precision in terms of cargo selection.

MATERIALS AND METHODS

Cells and viruses

HeLa and HEK293T (from the ATCC) were cultured in Dulbecco's modified Eagle's medium (DMEM) containing 10% fetal calf serum. Single cycle HIV-1 was generated by co-transfection of plasmids encoding the NL43 genome lacking the env gene and VSV-G protein into HEK293T cells. HeLa cells stably expressing GFP–MKLP1 were cultured in the above medium supplemented with 500 µg ml^{-1} G418.

Plasmids, siRNA and transfection

TRIM17 and Mcl-1 were PCR amplified from commercially available cDNA clones and recombined into pDONR221 using the BP reaction (Life Tech) prior to being recombined into pDest expression plasmids by LR cloning. All siRNA smart pools were from Dharmacon except siRNA TRIM17.2 and TRIM17.3, which were purchased from Qiagen. With the exception of the siRNA transfections for the TRIM screen (with siRNA pre-printed into the 96 well plates and transfected using Dharmafect reagent), siRNA was delivered to cells by nucleoporation (Amaxa). Sequence information for siRNA is found in Table S1. Plasmid transfections were performed by either $CaPO_4$ or nucleoporation (Amaxa). All other plasmids have been described previously (Mandell et al., 2014). Samples were prepared for analysis the day after DNA transfection. For siRNA experiments, samples were prepared 48 h after siRNA transfection with the exception of experiments assessing the effects of knockdown on cell cycle or midbodies. These experiments were performed 72 h after transfection.

Infection and treatments

Transfected HEK293T cells were exposed to virus at 4°C for 1 h to allow binding but not entry. Unbound virus was removed and bound virus was allowed to infect cells under starvation-induced autophagy conditions (EBSS) at 37°C for 3 h. Samples were then prepared for immunoblotting. Working concentrations for inhibitors were as follows: pp242, 10 µg ml^{-1}; bafilomycin A1, 60 ng ml^{-1}.

Quantitative RT-PCR

Cells were collected in RNALater (Qiagen, Valencia, CA). RNA was isolated and purified using RNeasy kits (Qiagen) and cDNA was generated by using a high capacity cDNA reverse transcriptase kit with RNase inhibitor and random hexamer primers (Applied Biosystems, Foster City, CA) on a GeneAmp PCR System 9700 thermocycler (Applied Biosystems). Quantitative real-time PCR (qPCR) was performed using an ViiA 7 real-time PCR system with the Taqman Gene Expression master mix (Applied Biosystems) and a Prime Time Predesigned qPCR Assay for *Trim17* (Integrated DNA technologies, Coralville, IA). Gene expression was quantified using ViiA 7 QuantStudio Software v1.2.4 (Applied Biosystems) relative to the housekeeping gene *Hprt*. The probe and primer set for *Trim17* is as follows; probe 5′-/56-FAM/TCCTTCAC-C/ZEN/TTGCCCTGCCA/3IAbkFQ/-3′ (Integrated DNA Technologies), forward primer 5′-CTTCTCAAACTCCAGCACAATG-3′, reverse primer 5′-AGTACCTTCGGGAGCAGAT-3′. The probe and primer set for *hprt* is as follows; probe 5′-/56-FAM/AGCCTAAGA/ZEN/TGAGAGTTCAAGT-TGAGTTTGG/3IAbkFQ/-3′ (Integrated DNA Technologies), forward primer 5′-GCGATGTCAATAGGACTCCAG-3′, reverse primer 5′-TTGTTGTA-GGATATGCCCTTGA-3′.

Immunoblotting, immunofluorescence microscopy and co-immunoprecipitation

Most immunoprecipitation, immunofluorescent labeling and immunoblots were performed as described previously (Kyei et al., 2009) using a NP-40-based buffer to generate protein lysates. Where indicated, cell lysis was performed with RIPA buffer containing 1% NP-40 and 0.1% SDS. Antibodies used were against: Flag (Sigma), p62 (BD), ULK1 phospho-Ser317 and phospho-Ser757 (Cell Signaling), GFP (Abcam), mCherry (Abcam), Mcl-1 (Abcam), Bcl-2 (Abcam), IFT20 (Abcam), OFD1 (Sigma), ZWINT (Pierce), actin (Abcam), ubiquitin (MBL), LC3B (Sigma and MBL), c-Myc (Santa Cruz), TFEB (Cell Signaling), and MKLP1 (Santa Cruz Biotechnology). Additional information about antibody usage is found in supplementary information (Table S2). All densitomentric quantitation of immunoblot signals was normalized to actin. Quantitative analysis of colocalization from confocal micrographs was performed using Slidebook 6 software (Intelligent Imaging).

High-content imaging

All high-content experiments were performed on HeLa cells in a 96-well plate format. Following the indicated treatments, cells were immunofluorescently labeled. High-content imaging and analysis was performed using a Cellomics HCS scanner and iDEV software (Thermo) and >500 cells were analyzed per treatment in quadruplicate per experiment. Cell outlines were automatically determined based on background nuclear staining. For experiments determining the total abundance of p62, the SpotDetector BioApp was used to measure total above-background fluorescence per cell. For assays involving the quantitation of defined puncta (e.g. p62 or midbodies) or determining the extent of colocalization, the Colocalization BioApp was used. When necessary, GFP-positive cell populations were selected as previously described (Mandell et al., 2014).

Flow cytometry

HeLa cells subjected to control or TRIM17 knockdown were culture for 72 h prior to paraformaldehyde fixation, permeabilization with Triton-X-100, RNAse A treatment and staining with propidium iodide

(0.5 µg ml^{-1}). Data was collected in the FL-2 channel using a BD FACScan instrument.

siRNA screen of TRIMs for roles in midbody degradation

HeLa cells stably expressing GFP-tagged MKLP1 were cultured in 96-well plates containing siRNA smart pools against a subset of human TRIMs (or control siRNAs) and transfection reagent (Dharmacon). At 72 h after plating, the cells were fixed with paraformaldehyde and stained with Hoechst 33342. High-content imaging of was performed as described above. Two separate experiments were carried out. TRIMs whose knockdowns increased the number of midbodies per cell by >3 s.d. above the mean of non-targeting siRNA controls in both experiments were considered hits.

Correlative-light electron microscopy

HeLa cells were transfected with GFP–TRIM17 and plated on gridded dishes (Mattek) prior to fixation with 1.5% glutaraldehyde and 2% paraformaldehyde. The location of GFP-positive cells on the grid was then notated prior to post-fixation treatment with 1% osmium tetroxide, dehydration with ethanol and resin embedding. Resin blocks were trimmed to expose the area of interest, and 70–90-nm sections were cut with a diamond knife, stained with uranyl acetate and lead citrate and examined using a Jeol 1400EX transmission electron microscope.

Statistical analysis

Two-tailed *t*-tests or ANOVA with Bonferroni *post hoc* analysis were used to test for statistical significance, which was taken as $P<0.05$ from three or more independent experiments.

Acknowledgements

We thank the Electron Microscopy Unit at the Institute of Biotechnology, University of Helsinki, for technical help and use of equipment. We acknowledge L.R. Mandell for technical assistance.

Competing interests

The authors declare no competing or financial interests.

Author contributions

M.A.M., T.A., S.K., M.J.C., and A.J. performed experiments and analyzed the data. M.A.M., R.P., E.L.-E., T.J., and V.D. designed and supervised experiments. M.A.M. and V.D. wrote the manuscript.

Funding

This work was supported by the National Institutes of Health [grant numbers AI042999 and AI111935 to V.D.]. E.L.-E. and T.A. were supported by the Suomen Akatemia (Academy of Finland) and the Magnus Ehrnroothin Säätiö (Magnus Ehrnrooth Foundation). Deposited in PMC for release after 12 months.

Supplementary information

Supplementary information available online at
http://jcs.biologists.org/lookup/doi/10.1242/jcs.190017.supplemental

References

Barde, I., Rauwel, B., Marin-Florez, R. M., Corsinotti, A., Laurenti, E., Verp, S., Offner, S., Marquis, J., Kapopoulou, A., Vanicek, J. et al. (2013). A KRAB/KAP1-miRNA cascade regulates erythropoiesis through stage-specific control of mitophagy. *Science* **340**, 350-353.

Birgisdottir, A. B., Lamark, T. and Johansen, T. (2013). The LIR motif - crucial for selective autophagy. *J. Cell Sci.* **126**, 3237-3247.

Bjørkøy, G., Lamark, T., Brech, A., Outzen, H., Perander, M., Øvervatn, A., Stenmark, H. and Johansen, T. (2005). p62/SQSTM1 forms protein aggregates degraded by autophagy and has a protective effect on huntingtin-induced cell death. *J. Cell Biol.* **171**, 603-614.

Bodemann, B. O., Orvedahl, A., Cheng, T., Ram, R. R., Ou, Y.-H., Formstecher, E., Maiti, M., Hazelett, C. C., Wauson, E. M., Balakireva, M. et al. (2011). RalB and the exocyst mediate the cellular starvation response by direct activation of autophagosome assembly. *Cell* **144**, 253-267.

Chang, N. C., Nguyen, M., Germain, M. and Shore, G. C. (2010). Antagonism of Beclin 1-dependent autophagy by BCL-2 at the endoplasmic reticulum requires NAF-1. *EMBO J.* **29**, 606-618.

Chauhan, S., Goodwin, J. G., Chauhan, S., Manyam, G., Wang, J., Kamat, A. M. and Boyd, D. D. (2013). ZKSCAN3 is a master transcriptional repressor of autophagy. *Mol. Cell* **50**, 16-28.

Criollo, A., Niso-Santano, M., Malik, S. A., Michaud, M., Morselli, E., Mariño, G., Lachkar, S., Arkhipenko, A. V., Harper, F., Pierron, G. et al. (2011). Inhibition of autophagy by TAB2 and TAB3. *EMBO J.* **30**, 4908-4920.

Dionne, L. K., Wang, X.-J. and Prekeris, R. (2015). Midbody: from cellular junk to regulator of cell polarity and cell fate. *Curr. Opin. Cell Biol.* **35**, 51-58.

Dooley, H. C., Razi, M., Polson, H. E., Girardin, S. E., Wilson, M. I. and Tooze, S. A. (2014). WIPI2 links LC3 conjugation with PI3P, autophagosome formation, and pathogen clearance by recruiting Atg12-5-16L1. *Mol. Cell* **55**, 238-252.

Egan, D. F., Shackelford, D. B., Mihaylova, M. M., Gelino, S., Kohnz, R. A., Mair, W., Vasquez, D. S., Joshi, A., Gwinn, D. M., Taylor, R. et al. (2011). Phosphorylation of ULK1 (hATG1) by AMP-activated protein kinase connects energy sensing to mitophagy. *Science* **331**, 456-461.

Endo, H., Ikeda, K., Urano, T., Horie-Inoue, K. and Inoue, S. (2012). Terf/TRIM17 stimulates degradation of kinetochore protein ZWINT and regulates cell proliferation. *J. Biochem.* **151**, 139-144.

Erlich, S., Mizrachy, L., Segev, O., Lindenboim, L., Zmira, O., Adi-Harel, S., Hirsch, J. A., Stein, R. and Pinkas-Kramarski, R. (2007). Differential interactions between Beclin 1 and Bcl-2 family members. *Autophagy* **3**, 561-568.

Frémont, S., Gérard, A., Galloux, M., Janvier, K., Karess, R. E. and Berlioz-Torrent, C. (2013). Beclin-1 is required for chromosome congression and proper outer kinetochore assembly. *EMBO Rep.* **14**, 364-372.

Fulda, S. and Kögel, D. (2015). Cell death by autophagy: emerging molecular mechanisms and implications for cancer therapy. *Oncogene* **34**, 5105-5113.

Germain, M., Nguyen, A. P., Le Grand, J. N., Arbour, N., Vanderluit, J. L., Park, D. S., Opferman, J. T. and Slack, R. S. (2011). MCL-1 is a stress sensor that regulates autophagy in a developmentally regulated manner. *EMBO J.* **30**, 395-407.

Gomes, L. C. and Dikic, I. (2014). Autophagy in antimicrobial immunity. *Mol. Cell* **54**, 224-233.

Imam, S., Talley, S., Nelson, R. S., Dharan, A., O'connor, C., Hope, T. J. and Campbell, E. M. (2016). TRIM5alpha degradation via autophagy is not required for retroviral restriction. *J. Virol.* **90**, 3400-3410.

Isakson, P., Lystad, A. H., Breen, K., Koster, G., Stenmark, H. and Simonsen, A. (2013). TRAF6 mediates ubiquitination of KIF23/MKLP1 and is required for midbody ring degradation by selective autophagy. *Autophagy* **9**, 1955-1964.

Johansen, T. and Lamark, T. (2011). Selective autophagy mediated by autophagic adapter proteins. *Autophagy* **7**, 279-296.

Katsuragi, Y., Ichimura, Y. and Komatsu, M. (2015). p62/SQSTM1 functions as a signaling hub and an autophagy adaptor. *FEBS J.* **282**, 4672-4678.

Khaminets, A., Heinrich, T., Mari, M., Grumati, P., Huebner, A. K., Akutsu, M., Liebmann, L., Stolz, A., Nietzsche, S., Koch, N. et al. (2015). Regulation of endoplasmic reticulum turnover by selective autophagy. *Nature* **522**, 354-358.

Kihara, A., Noda, T., Ishihara, N. and Ohsumi, Y. (2001). Two distinct Vps34 phosphatidylinositol 3-kinase complexes function in autophagy and carboxypeptidase Y sorting in Saccharomyces cerevisiae. *J. Cell Biol.* **152**, 519-530.

Kim, J., Kundu, M., Viollet, B. and Guan, K.-L. (2011). AMPK and mTOR regulate autophagy through direct phosphorylation of Ulk1. *Nat. Cell Biol.* **13**, 132-141.

Kim, J., Kim, Y. C., Fang, C., Russell, R. C., Kim, J. H., Fan, W., Liu, R., Zhong, Q. and Guan, K.-L. (2013). Differential regulation of distinct Vps34 complexes by AMPK in nutrient stress and autophagy. *Cell* **152**, 290-303.

Kimura, T., Jain, A., Choi, S. W., Mandell, M. A., Schroder, K., Johansen, T. and Deretic, V. (2015). TRIM-mediated precision autophagy targets cytoplasmic regulators of innate immunity. *J. Cell Biol.* **210**, 973-989.

Kimura, T., Mandell, M. and Deretic, V. (2016). Precision autophagy directed by receptor regulators-emerging examples within the TRIM family. *J. Cell Sci.* **129**, 881-891.

Klionsky, D. J., Abdelmohsen, K., Abe, A., Abedin, M. J., Abeliovich, H., Acevedo Arozena, A., Adachi, H., Adams, C. M., Adams, P. D., Adeli, K. et al. (2016). Guidelines for the use and interpretation of assays for monitoring autophagy (3rd edition). *Autophagy* **12**, 1-222.

Kuo, T.-C., Chen, C.-T., Baron, D., Onder, T. T., Loewer, S., Almeida, S., Weismann, C. M., Xu, P., Houghton, J.-M., Gao, F.-B. et al. (2011). Midbody accumulation through evasion of autophagy contributes to cellular reprogramming and tumorigenicity. *Nat. Cell Biol.* **13**, 1214-1223.

Kyei, G. B., Dinkins, C., Davis, A. S., Roberts, E., Singh, S. B., Dong, C., Wu, L., Kominami, E., Ueno, T., Yamamoto, A. et al. (2009). Autophagy pathway intersects with HIV-1 biosynthesis and regulates viral yields in macrophages. *J. Cell Biol.* **186**, 255-268.

Lazarou, M., Sliter, D. A., Kane, L. A., Sarraf, S. A., Wang, C., Burman, J. L., Sideris, D. P., Fogel, A. I. and Youle, R. J. (2015). The ubiquitin kinase PINK1 recruits autophagy receptors to induce mitophagy. *Nature* **524**, 309-314.

Liang, X. H., Jackson, S., Seaman, M., Brown, K., Kempkes, B., Hibshoosh, H. and Levine, B. (1999). Induction of autophagy and inhibition of tumorigenesis by beclin 1. *Nature* **402**, 672-676.

Lindqvist, L. M., Heinlein, M., Huang, D. C. S. and Vaux, D. L. (2014). Prosurvival Bcl-2 family members affect autophagy only indirectly, by inhibiting Bax and Bak. *Proc. Natl. Acad. Sci. USA* **111**, 8512-8517.

Magiera, M. M., Mora, S., Mojsa, B., Robbins, I., Lassot, I. and Desagher, S. (2013). Trim17-mediated ubiquitination and degradation of Mcl-1 initiate apoptosis in neurons. *Cell Death Differ.* **20**, 281-292.

Mandell, M. A., Jain, A., Arko-Mensah, J., Chauhan, S., Kimura, T., Dinkins, C., Silvestri, G., Münch, J., Kirchhoff, F., Simonsen, A. et al. (2014). TRIM proteins regulate autophagy and can target autophagic substrates by direct recognition. *Dev. Cell* **30**, 394-409.

Matsunaga, K., Saitoh, T., Tabata, K., Omori, H., Satoh, T., Kurotori, N., Maejima, I., Shirahama-Noda, K., Ichimura, T., Isobe, T. et al. (2009). Two Beclin 1-binding proteins, Atg14L and Rubicon, reciprocally regulate autophagy at different stages. *Nat. Cell Biol.* **11**, 385-396.

Mizushima, N. and Komatsu, M. (2011). Autophagy: renovation of cells and tissues. *Cell* **147**, 728-741.

Mizushima, N., Yoshimori, T. and Ohsumi, Y. (2011). The role of atg proteins in autophagosome formation. *Annu. Rev. Cell Dev. Biol.* **27**, 107-132.

Niida, M., Tanaka, M. and Kamitani, T. (2010). Downregulation of active IKK beta by Ro52-mediated autophagy. *Mol. Immunol.* **47**, 2378-2387.

Obara, K., Sekito, T., Niimi, K. and Ohsumi, Y. (2008). The Atg18-Atg2 complex is recruited to autophagic membranes via phosphatidylinositol 3-phosphate and exerts an essential function. *J. Biol. Chem.* **283**, 23972-23980.

Pampliega, O., Orhon, I., Patel, B., Sridhar, S., Díaz-CARRETERO, A., Beau, I., Codogno, P., Satir, B. H., Satir, P. and Cuervo, A. M. (2013). Functional interaction between autophagy and ciliogenesis. *Nature* **502**, 194-200.

Pan, J.-A., Sun, Y., Jiang, Y.-P., Bott, A. J., Jaber, N., Dou, Z., Yang, B., Chen, J.-S., Catanzaro, J. M., Du, C. et al. (2016). TRIM21 ubiquitylates SQSTM1/p62 and suppresses protein sequestration to regulate redox homeostasis. *Mol. Cell* **61**, 720-733.

Pankiv, S., Clausen, T. H., Lamark, T., Brech, A., Bruun, J.-A., Outzen, H., Øvervatn, A., Bjørkøy, G. and Johansen, T. (2007). p62/SQSTM1 binds directly to Atg8/LC3 to facilitate degradation of ubiquitinated protein aggregates by autophagy. *J. Biol. Chem.* **282**, 24131-24145.

Pattingre, S., Tassa, A., Qu, X., Garuti, R., Liang, X. H., Mizushima, N., Packer, M., Schneider, M. D. and Levine, B. (2005). Bcl-2 antiapoptotic proteins inhibit Beclin 1-dependent autophagy. *Cell* **122**, 927-939.

Pertel, T., Hausmann, S., Morger, D., Züger, S., Guerra, J., Lascano, J., Reinhard, C., Santoni, F. A., Uchil, P. D., Chatel, L. et al. (2011). TRIM5 is an innate immune sensor for the retrovirus capsid lattice. *Nature* **472**, 361-365.

Pineda, C. T., Ramanathan, S., Fon Tacer, K., Weon, J. L., Potts, M. B., Ou, Y.-H., White, M. A. and Potts, P. R. (2015). Degradation of AMPK by a cancer-specific ubiquitin ligase. *Cell* **160**, 715-728.

Pohl, C. and Jentsch, S. (2009). Midbody ring disposal by autophagy is a post-abscission event of cytokinesis. *Nat. Cell Biol.* **11**, 65-70.

Popelka, H. and Klionsky, D. J. (2015). Post-translationally-modified structures in the autophagy machinery: an integrative perspective. *FEBS J.* **282**, 3474-3488.

Randow, F. and Youle, R. J. (2014). Self and nonself: how autophagy targets mitochondria and bacteria. *Cell Host Microbe* **15**, 403-411.

Reymond, A., Meroni, G., Fantozzi, A., Merla, G., Cairo, S., Luzi, L., Riganelli, D., Zanaria, E., Messali, S., Cainarca, S. et al. (2001). The tripartite motif family identifies cell compartments. *EMBO J.* **20**, 2140-2151.

Rogov, V., Dötsch, V., Johansen, T. and Kirkin, V. (2014). Interactions between autophagy receptors and ubiquitin-like proteins form the molecular basis for selective autophagy. *Mol. Cell* **53**, 167-178.

Russell, R. C., Tian, Y., Yuan, H., Park, H. W., Chang, Y.-Y., Kim, J., Kim, H., Neufeld, T. P., Dillin, A. and Guan, K.-L. (2013). ULK1 induces autophagy by phosphorylating Beclin-1 and activating VPS34 lipid kinase. *Nat. Cell Biol.* **15**, 741-750.

Settembre, C., Di Malta, C., Polito, V. A., Garcia Arencibia, M., Vetrini, F., Erdin, S., Erdin, S. U., Huynh, T., Medina, D., Colella, P. et al. (2011). TFEB links autophagy to lysosomal biogenesis. *Science* **332**, 1429-1433.

Settembre, C., Zoncu, R., Medina, D. L., Vetrini, F., Erdin, S., Huynh, T., Ferron, M., Karsenty, G., Vellard, M. C., Facchinetti, V. et al. (2012). A lysosome-to-nucleus signalling mechanism senses and regulates the lysosome via mTOR and TFEB. *EMBO J.* **31**, 1095-1108.

Shi, C. S. and Kehrl, J. H. (2010). TRAF6 and A20 regulate lysine 63-linked ubiquitination of Beclin-1 to control TLR4-induced autophagy. *Sci. Signal* **3**, ra42.

Stolz, A., Ernst, A. and Dikic, I. (2014). Cargo recognition and trafficking in selective autophagy. *Nat. Cell Biol.* **16**, 495-501.

Stremlau, M., Owens, C. M., Perron, M. J., Kiessling, M., Autissier, P. and Sodroski, J. (2004). The cytoplasmic body component TRIM5alpha restricts HIV-1 infection in Old World monkeys. *Nature* **427**, 848-853.

Tai, W.-T., Shiau, C.-W., Chen, H.-L., Liu, C.-Y., Lin, C.-S., Cheng, A.-L., Chen, P.-J. and Chen, K.-F. (2013). Mcl-1-dependent activation of Beclin 1 mediates autophagic cell death induced by sorafenib and SC-59 in hepatocellular carcinoma cells. *Cell Death Dis.* **4**, e485.

Takaesu, G., Kobayashi, T. and Yoshimura, A. (2012). TGFbeta-activated kinase 1 (TAK1)-binding proteins (TAB) 2 and 3 negatively regulate autophagy. *J. Biochem.* **151**, 157-166.

Tang, Z., Lin, M. G., Stowe, T. R., Chen, S., Zhu, M., Stearns, T., Franco, B. and Zhong, Q. (2013). Autophagy promotes primary ciliogenesis by removing OFD1 from centriolar satellites. *Nature* **502**, 254-257.

Urano, T., Usui, T., Takeda, S., Ikeda, K., Okada, A., Ishida, Y., Iwayanagi, T., Otomo, J., Ouchi, Y. and Inoue, S. (2009). TRIM44 interacts with and stabilizes terf, a TRIM ubiquitin E3 ligase. *Biochem. Biophys. Res. Commun.* **383**, 263-268.

Wei, Y., Pattingre, S., Sinha, S., Bassik, M. and Levine, B. (2008). JNK1-mediated phosphorylation of Bcl-2 regulates starvation-induced autophagy. *Mol. Cell* **30**, 678-688.

Wei, Y., An, Z., Zou, Z., Sumpter, R., Su, M., Zang, X., Sinha, S., Gaestel, M. and Levine, B. (2015). The stress-responsive kinases MAPKAPK2/MAPKAPK3 activate starvation-induced autophagy through Beclin 1 phosphorylation. *Elife* **4**, e05289.

Yang, Y., Fiskus, W., Yong, B., Atadja, P., Takahashi, Y., Pandita, T. K., Wang, H.-G. and Bhalla, K. N. (2013). Acetylated hsp70 and KAP1-mediated Vps34 SUMOylation is required for autophagosome creation in autophagy. *Proc. Natl. Acad. Sci. USA* **110**, 6841-6846.

Zhong, Y., Wang, Q. J., Li, X., Yan, Y., Backer, J. M., Chait, B. T., Heintz, N. and Yue, Z. (2009). Distinct regulation of autophagic activity by Atg14L and Rubicon associated with Beclin 1-phosphatidylinositol-3-kinase complex. *Nat. Cell Biol.* **11**, 468-476.